Arch Appl Mech (2008) 78: 295–309
DOI 10.1007/s00419-007-0161-x

ORIGINAL

B. Li · Y. W. Liu · Q. H. Fang

Interaction of an anti-plane singularity with interfacial anti-cracks in cylindrically anisotropic composites

Received: 25 February 2007 / Accepted: 2 July 2007 / Published online: 10 August 2007

Abstract Anti-plane problem for a singularity interacting with interfacial anti-cracks (rigid lines) under uniform shear stress at infinity in cylindrically anisotropic composites is investigated by utilizing a complex potential technique in this paper. After obtaining the general solution for this problem, the closed solution for the interface containing one anti-crack is presented analytically. In addition, the complex potentials for a screw dislocation dipole inside matrix are obtained by the superimposing method. Expressions of stress singularities around the anti-crack tips, image forces and torques acting on the dislocation or the center of dipole are given explicitly. The results indicate that the anisotropy properties of materials may weaken the stress singularity near the anti-crack tip for the singularity being a concentrated force but enhance the one for the singularity being a screw dislocation and change the equilibrium position of screw dislocation. The presented solutions are valid for anisotropic, orthotropic or isotropic composites and can be reduced to some new or previously known results.

Keywords Anti-plane problem · Interface anti-cracks · Cylindrically anisotropic composites

1 Introduction

The study of singularities (including concentrated forces and dislocations) interacting with interfacial cracks and anti-cracks, which can be produced inevitably in manufacturing and the production of composite materials, as well as mechanics and materials science, is motivated by the need of a better understanding of the mechanism of strengthening and toughening of materials. Due to its importance, this problem has received much attention during the last several decades. For the anti-crack problem, we have provided some examples of early contributions [1–9]. Recently, Wu and Du [10] developed an effective method to investigate the elastic field and electric field of a rigid line in a confocal elliptic piezoelectric inhomogeneity embedded in an infinite piezoelectric medium. Electro-elastic interaction between a semi-infinite anti-crack and a screw dislocation under anti-plane mechanical and in-plane electrical loading was carried out by Chen et al. [11]. Xiao et al. [12] proposed a dislocation of the pileup model for micro-crack initiation at the rigid line inhomogeneity tip based on Zener–Stroh crack initiation mechanism. Using the complex variable method, Liu and Fang [13] investigated the electro-elastic interaction between a piezoelectric screw dislocation and circular interfacial rigid lines. Fang et al. [14] dealt with the interaction of a generalized screw dislocation with circular-arc interfacial rigid lines under remote anti-plane shear stresses, in-plane electric and magnetic loads in linear magnetoelectroelastic materials. A dislocation emission mechanism for micro-crack initiation at the tip of a semi-infinite rigid line inhomogeneity in a piezoelectric solid was considered by Xiao et al. [15]. Applying a

B. Li · Y. W. Liu (✉) · Q. H. Fang
College of Mechanics and Aerospace, Hunan University, Changsha 410082, China
E-mail: liuyouw8294@sina.com
Tel.: +86-731-8821889
Fax: +86-731-8822330

complex variable method and conformal mapping technique, Prasad et al. [16] obtained the Green's functions for a point force and dislocation interacting with interfacial elliptical rigid inclusion in a bonded bimaterial system and examined the problem of an internal crack or thin rigid line interacting with the interfacial inclusion. Xiao et al. [17] derived an analytical closed-form solution for a screw dislocation interacting with collinear rigid lines along the interface of two dissimilar piezoelectric media.

For cylindrically anisotropic materials, Yang and Yuan [18] studied the anti-plane shear problem of a dissimilar interfacial circular crack in cylindrically anisotropic solids. Ting [19] investigated the problem of a circular tube subjected to a uniform normal stress and shearing stresses at the inner and outer surfaces or the tube. A wedge of cylindrically anisotropic material under anti-plane deformation was considered by Ting [20].

This paper attempts to investigate the interaction between an anti-plane singularity and interfacial anti-cracks in cylindrically anisotropic composites by utilizing complex potential technique. The closed solution for interface containing one anti-crack is presented analytically. In addition, the complex potentials for a screw dislocation dipole inside matrix are obtained by superimposing method. Stress singularities around the anti-crack tips, image forces and torques acting on dislocation or the center of dipole are given explicitly. In the final, the influences of materials' anisotropies upon the stress singularities and image forces are discussed by numerical method. It should be pointed out that the presented solutions in this paper are valid for anisotropic, orthotropic or isotropic composites and can be reduced to some novel or previously known results.

2 Basic formulation and problem description

For a cylindrically anisotropic anti-plane problem, the equilibrium equation can be given as

$$c_{55}\left(\frac{\partial^2 u_3}{\partial r^2}+\frac{1}{r}\frac{\partial u_3}{\partial r}\right)+2c_{45}\frac{1}{r}\frac{\partial^2 u_3}{\partial r\partial\theta}+c_{44}\frac{1}{r^2}\frac{\partial^2 u_3}{\partial\theta^2}=0 \tag{1}$$

where $u_3 = u_3(r,\theta)$ is the out-of-plane displacement, and c_{44}, c_{45} and c_{55} are the elastic constants of the material. The shear stresses σ_{3r} and $\sigma_{3\theta}$ are related to the displacement u_3 by the generalized Hooke's law

$$\sigma_{3r} = c_{45}\frac{1}{r}\frac{\partial u_3}{\partial\theta}+c_{55}\frac{\partial u_3}{\partial r} \tag{2}$$

$$\sigma_{3\theta} = c_{44}\frac{1}{r}\frac{\partial u_3}{\partial\theta}+c_{45}\frac{\partial u_3}{\partial r}. \tag{3}$$

The general solution of Eq. (1) may be expressed in terms of a single holomorphic function $\varphi(\xi)$ as follows:

$$u_3(r,\theta) = \mathrm{Re}[\varphi(\xi)] \tag{4}$$

where Re denotes the real part, and a new argument ξ is defined as [18]

$$xi = \left(\frac{r}{a}\right)^{-i\mu-1} re^{i\theta} \tag{5}$$

where $i=\sqrt{-1}$, and a is a characteristic length designated here as the radius of the circular arc. The μ are roots of the following algebraic characteristic equation

$$c_{55}\mu^2-2c_{45}\mu+c_{44}=0. \tag{6}$$

The roots of Eq. (6) are either complex of purely imaginary but cannot be real. Without loss of generality, μ is chosen as

$$\mu=\frac{c_{45}}{c_{55}}+\frac{i\sqrt{c_{44}c_{55}-c_{45}^2}}{c_{55}} \tag{7}$$

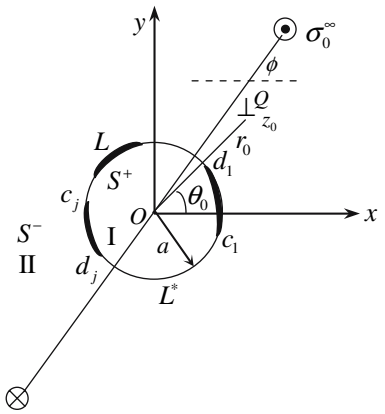

Fig. 1 An antiplane singularity interacting with interfacial anti-cracks model

where $\mathrm{Re}(-i\mu) = \sqrt{c_{44}c_{55} - c_{45}^2}/c_{55} > 0$. When the material is isotropic, μ becomes i. It is expedient to define $\Phi(\xi) = \mathrm{d}\varphi(\xi)/\mathrm{d}\xi$ so that stress components may be written as

$$\sigma_{3r} = \frac{1}{r}\,\mathrm{Re}[\beta\xi\Phi(\xi)] \tag{8}$$

$$\sigma_{3\theta} = \frac{1}{r}\,\mathrm{Re}[\mu\beta\xi\Phi(\xi)] \tag{9}$$

where $\beta = \sqrt{c_{44}c_{55} - c_{45}^2}$.

Here we also give the derivative of displacement with respect to θ in that it will be adopted in the following text

$$\frac{\partial u_3}{\partial\theta} = \mathrm{Re}[i\xi\Phi(\xi)]. \tag{10}$$

The problem to consider is as follows. Referring to Fig. 1, we embed a cylindrical inhomogeneity (region S^+) of radius a in an infinite matrix (region S^-). The media interior to and exterior to the circle are cylindrically anisotropic elastic solids with dissimilar material properties from each other. A singularity containing a screw dislocation with Burgers vector b and a anti-plane concentrated force p is located at arbitrary point $z_0(= r_0\mathrm{e}^{i\theta_0})$ inside matrix. Anti-plane uniform shear stress σ_0^∞, which makes an angle ϕ with the x-axis, is applied at infinite. A series of anti-cracks (namely, rigid lines) lie along a part L of the interface between the inhomogeneity and matrix, where L is a union of anti-cracks L_j with the tips c_j and $d_j (j = 1, 2, \ldots, n)$. L^* is the remainder of the interface along which the inhomogeneity and the matrix are perfectly bonded.

The boundary conditions along $z = a\mathrm{e}^{i\theta}$ for the present problem can be expressed as

$$u_{3(1)}^+ = u_{3(2)}^- = \delta_j \qquad (j = 1, 2, \ldots, n) \quad \text{on } L \tag{11}$$

$$\sigma_{3r(1)}^+ = \sigma_{3r(2)}^- \quad \text{on } L^* \tag{12}$$

$$u_{3(1)}^+ = u_{3(2)}^- \quad \text{on } L^* \tag{13}$$

where δ_j denotes a small anti-plane displacement of any anti-crack L_j, the subscripts 1 and 2 denote the quantities defined in the regions S^+ and S^-, with the superscripts + and – used to representing the boundary values of the physical quantities as they are approached from S^+ and S^-, respectively.

From Eq. (11), we have

$$\left[\frac{\partial u_{3(1)}}{\partial\theta}\right]^+ + \left[\frac{\partial u_{3(2)}}{\partial\theta}\right]^- = 0 \,\text{on} \quad L \tag{14}$$

$$\left[\frac{\partial u_{3(1)}}{\partial\theta}\right]^+ - \left[\frac{\partial u_{3(2)}}{\partial\theta}\right]^- = 0 \quad \text{on } L. \tag{15}$$

From Eq. (13), we obtain

$$\left[\frac{\partial u_{3(1)}}{\partial \theta}\right]^{+} = \left[\frac{\partial u_{3(2)}}{\partial \theta}\right]^{-} \quad \text{on } L^{*}. \tag{16}$$

3 General solution of problem

Referring to the works by Suo [21], Kattis and Providas [22] and Lee et al. [23], the generalized analytical function $\Phi_1(\xi_1)$ and $\Phi_2(\xi_2)$ in the region S^+ and S^- under considerations can be, respectively, written as

$$\Phi_1(\xi_1) = D + \Phi_{10}(\xi_1) \quad \xi_1 \in S^+ \tag{17}$$

$$\Phi_2(\xi_2) = \frac{Q}{\xi_2 - \xi_0} + \Gamma + \Phi_{20}(\xi_2) \quad \xi_2 \in S^- \tag{18}$$

where $\xi_k = (\frac{r}{a})^{-i\mu_k - 1} r\mathrm{e}^{i\theta} (k = 1, 2), \xi_0 = (\frac{r_0}{a})^{-i\mu - 1} r\mathrm{e}^{i\theta_0}$ (here, $\mu = \mu_2$ for ξ_0 in the matrix) and $Q = \frac{b}{2\pi i} - \frac{p}{2\pi\beta}$, D is a complex constant to be determined and $\Phi_{10}(\xi_1) = \mathrm{O}(1/\xi_1)$ near $\xi_1 = 0, \Phi_{20}(\xi_2)$ is holomorphic in the region S^- and vanishes at infinity, Γ is determined from the loads at infinity.

$$\Gamma = \sigma_0 \mathrm{e}^{-i\phi}/\beta_2. \tag{19}$$

Noting that on the interface $\xi = z = a\mathrm{e}^{i\theta}$, one can translate the procedure derivation of the function with argument $\xi_k (k = 1, 2)$ into the corresponding function with argument $z = r\mathrm{e}^{i\theta}$.

Applying Riemann–Schwarz's symmetry principle, we extend the definition of the holomorphic function $\Phi_1(z)$ and $\Phi_2(z)$ into region S^- and S^+, respectively, through L by

$$\Phi_k(z) = \frac{a^2}{z^2} \bar{\Phi}_k \left(\frac{a^2}{z}\right) \quad (k = 1, 2). \tag{20}$$

Inserting Eq. (17) into Eq. (20), for large value of $|z|$, we get

$$\Phi_1(z) = \frac{a^2}{z^2} \bar{D} + \mathrm{O}\left(\frac{1}{z^3}\right) \quad z \in S^-. \tag{21}$$

Similarly, substituting Eq. (18) into Eq. (20) yields

$$\Phi_2(z) = -\bar{Q}\left(\frac{1}{z - z^*} - \frac{1}{z}\right) + \frac{a^2}{z^2}\bar{\Gamma} + \Phi_{20}(z) \quad z \in S^+ \tag{22}$$

where $z^* = a^2/\bar{z}_0$, where $z^* = a^2/\bar{z}_0$, $\Phi_{20}(z)$ is holomorphic in the region S^+.

From Eqs. (15) and (16), it is found that

$$\left[\frac{\partial u_{3(1)}}{\partial \theta}\right]^{+} = \left[\frac{\partial u_{3(2)}}{\partial \theta}\right]^{-} \quad z \in L + L^{*}. \tag{23}$$

Inserting Eq. (10) into Eq. (23) and noting Eq. (20) yield

$$[\Phi_1(z) + \Phi_2(z)]^{+} = [\Phi_2(z) + \Phi_1(z)]^{-} \quad z \in L + L^{*}. \tag{24}$$

According to the generalized Liouville's theorem, Eq. (24) leads to

$$\Phi_1(z)+\Phi_2(z)=\frac{Q}{z-z_0}-\bar{Q}\left(\frac{1}{z-z^*}-\frac{1}{z}\right)+\Gamma+\frac{a^2}{z^2}\bar{\Gamma}. \tag{25}$$

Substituting Eq. (8) into Eq. (12) and noting Eq. (20) yield

$$\beta_1\left[\Phi_1^+(z)+\Phi_1^-(z)\right]=\beta_2\left[\Phi_2^-(z)+\Phi_2^+(z)\right]\quad z\in L^*. \tag{26}$$

Inserting Eq. (25) into Eq. (26), it is found

$$\Phi_1^+(z)+\Phi_1^-(z)=h(z)\quad z\in L^* \tag{27}$$

where $h(z)=2m\cdot\left[\frac{Q}{z-z_0}-\bar{Q}\left(\frac{1}{z-z^*}-\frac{1}{z}\right)+\Gamma+\frac{a^2}{z^2}\bar{\Gamma}\right]$ with $m=\beta_2/(\beta_1+\beta_2)$.

According to Muskhelishvili [24], the general solution of Eq. (27) can be written as

$$\Phi_1(z)=\frac{X_0(z)}{2\pi i}\int\limits_{L^*}\frac{h(t)\mathrm{d}t}{X_0^+(t)(t-z)}+X_0(z)P_n(z) \tag{28}$$

where

$$P(z)=C_1z^{n-1}+C_2z^{n-2}+\cdots+C_n \tag{29}$$

$$X_0(z)=\prod_{j=1}^{n}(z-c_j)^{-1/2}(z-d_j)^{-1/2} \tag{30}$$

$X_0(z)$ is a single-valued branch in the plane cut along with L^* and for which $\lim\limits_{|z|\to\infty}z^nX_0(z)=1$.

After calculating the Cauchy integral in Eq. (27), we have

$$\Phi_1(z)=X_0(z)\left\{P_n(z)-\frac{1}{2}[h_0(z)+h_\infty(z)+h_{z_0}(z)+h_{z^*}(z)]\right\}+\frac{1}{2}h(z) \tag{31}$$

where $h_0(z)$, $h_\infty(z)$, $h_{z_0}(z)$ and $h_{z^*}(z)$ represent the principal parts at the points $z=0$, $z=\infty$, $z=z_0$ and $z=z^*$ of function $h(z)/X_0(z)$, respectively.

The remaining integration constants $C_{n-1},\ldots,C_0$ in Eq. (29) are determined from the equilibrium conditions of anti-cracks. Assuming that anti-cracks are external traction free, one has

$$\int\limits_{c_j}^{d_j}\frac{\sigma_{3r(1)}^+}{z}\mathrm{d}z-\int\limits_{c_j}^{d_j}\frac{\sigma_{3r(2)}^-}{z}\mathrm{d}z=0\qquad(j=1,2,\ldots,n)\quad z\in L_j. \tag{32}$$

Substituting Eq. (8) into Eq. (32) and noting Eq. (25) yield

$$\int\limits_{\Lambda_j}\left[(\beta_1-\beta_2)\Phi_1(z)+\beta_2\left[\frac{Q}{z-z_0}-\bar{Q}\left(\frac{1}{z-z^*}-\frac{1}{z}\right)+\Gamma+\frac{a^2}{z^2}\bar{\Gamma}\right]\right]\mathrm{d}z=0\quad(j=1,2,\ldots,n) \tag{33}$$

where Λ_j is a closed contour encircling each anti-crack L_j. The set of n linear algebraic equations given by Eq. (33) determine solely n remaining complex integration constants. Once $\Phi_1(z)$ is available, $\Phi_2(z)$ will be simply obtained from Eq. (25).

Replacing the argument z of functions $\Phi_1(z)$ and $\Phi_2(z)$ by ξ_k, the complete functions of $\Phi_1(\xi_1)$ and $\Phi_2(\xi_2)$ can be obtained [18].

4 Closed form solution for typical case

Consider the case of the interface with a single anti-crack and uniform shear loads at infinity. Without loss of generality, assume an interfacial anti-crack symmetrically placed with respect to the x-axis and the tips of which are located at $c_1 = a\mathrm{e}^{-i\alpha}$ and $d_1 = a\mathrm{e}^{i\alpha}$.

In this case, we have

$$P_1(z) = C_1, \quad X_0(z) = (z^2 - 2az\cos\alpha + a^2)^{-1/2}. \tag{34}$$

Expanding $1/X_0(z)$ into Laurent series in the vicinity of $z = 0$ and $|z| = \infty$, and noting $X_0(0) = 1/a$, it is found

$$h_0(z) = 2m \cdot \left[\frac{\bar{Q}a}{z} + \frac{a^3}{z^2}\bar{\Gamma} - \frac{a^2}{z}\bar{\Gamma}\cos\alpha\right], \tag{35a}$$

$$h_\infty(z) = 2m \cdot [Q + \Gamma z - \Gamma a\cos\alpha], \tag{35b}$$

$$h_{z_0}(z) = \frac{2mQ}{(z - z_0)X_0(z_0)}, \tag{35c}$$

$$h_{z^*}(z) = -\frac{2m\bar{Q}}{(z - z^*)X_0(z^*)}. \tag{35d}$$

Substituting Eq. (31) into Eq. (33) and noting Eqs. (34) and (35), one can derive C_1 by residue theorem.

$$C_1 = 0. \tag{36}$$

Replacing the argument z of functions $\Phi_1(z)$ and $\Phi_2(z)$ by ξ_k and considering Eqs. (25),(31) and (34)–(36), we obtain

$$\begin{aligned}\Phi_1(\xi_1) = {} & m\left[\frac{Q}{\xi_1 - \xi_0} - \frac{\bar{Q}}{\xi_1 - \xi^*} + \frac{\bar{Q}}{\xi_1}\right] - m\left[\frac{Q}{(\xi_1 - \xi_0)X_0(\xi_0)} - \frac{\bar{Q}}{(\xi_1 - \xi^*)X_0(\xi^*)} + \frac{\bar{Q}a}{\xi_1} + Q\right]X_0(\xi_1) \\ & -m\left(\Gamma\xi_1 - \Gamma a\cos\alpha + \frac{a^3}{\xi_1^2}\bar{\Gamma} - \frac{a^2}{\xi_1}\bar{\Gamma}\cos\alpha\right)X_0(\xi_1) + m\left(\Gamma + \frac{a^2}{\xi_1^2}\bar{\Gamma}\right)\end{aligned} \tag{37}$$

$$\begin{aligned}\Phi_2(\xi_2) = {} & \frac{m\beta_1}{\beta_2}\left[\frac{Q}{\xi_2 - \xi_0} - \frac{\bar{Q}}{\xi_2 - \xi^*} + \frac{\bar{Q}}{\xi_2}\right] + m\left[\frac{Q}{(\xi_2 - \xi_0)X_0(\xi_0)} - \frac{\bar{Q}}{(\xi_2 - \xi^*)X_0(\xi^*)} + \frac{\bar{Q}a}{\xi_2} + Q\right]X_0(\xi_2) \\ & +m\left(\Gamma\xi_2 - \Gamma a\cos\alpha + \frac{a^3}{\xi_2^2}\bar{\Gamma} - \frac{a^2}{\xi_2}\bar{\Gamma}\cos\alpha\right)X_0(\xi_2) + \frac{m\beta_1}{\beta_2}\left(\Gamma + \frac{a^2}{\xi_2^2}\bar{\Gamma}\right)\end{aligned} \tag{38}$$

where $\xi^* = a^2/\bar{\xi}_0$.

Assuming $Q = 0$, the new solution for two dissimilar cylindrically anisotropic solids interface containing an anti-crack under anti-plane shear at infinity can be simply derived from Eqs. (37) and (38). Setting $\beta_1 = \beta_2$, we give the complex potential of corresponding homogeneity material containing a single anti-crack as

$$\Phi(\xi) = \frac{1}{2}\left[\frac{Q}{\xi - \xi_0} - \frac{\bar{Q}}{\xi - \xi^*} + \frac{\bar{Q}}{\xi}\right] - \frac{1}{2}\left[\frac{Q}{(\xi - \xi_0)X_0(\xi_0)} - \frac{\bar{Q}}{(\xi - \xi^*)X_0(\xi^*)} + \frac{\bar{Q}a}{\xi} + Q\right]X_0(\xi)$$
$$-\frac{1}{2}\left(\Gamma\xi - \Gamma a\cos\alpha + \frac{a^3}{\xi^2}\bar{\Gamma} - \frac{a^2}{\xi}\bar{\Gamma}\cos\alpha\right)X_0(\xi) + \frac{1}{2}\left(\Gamma + \frac{a^2}{\xi^2}\bar{\Gamma}\right). \tag{39}$$

To our knowledge, this also is a novel result.

Furthermore, assuming $\alpha = 0$, namely, the interface anti-crack vanishes, one can reduce Eqs. (37) and (38) to

$$\Phi_1(\xi_1) = \frac{2mQ}{\xi_1 - \xi_0} + 2m\Gamma \tag{40}$$

$$\Phi_2(\xi_2) = \frac{Q}{\xi_2 - \xi_0} + \frac{m(\beta_2 - \beta_1)\bar{Q}}{\beta_2}\left(\frac{1}{\xi_2 - \xi^*} - \frac{1}{\xi_2}\right) + \Gamma - \frac{m(\beta_2 - \beta_1)}{\beta_2}\frac{a^2}{\xi_2^2}\bar{\Gamma}. \tag{41}$$

When the symmetries of materials are restricted to the crystal system with the symmetry higher than the orthotropy and $\Gamma = 0$, Eqs. (40) and (41) are in agreement with the work of Shin and Earmme [25].

If the matrix and inhomogeneity are two different isotropic materials, that is, $c_{44} = c_{55}, c_{45} = 0$, then $\beta = c_{44}, \xi = z$, it can be found from Eqs. (40) and (41),

$$\Phi_1(z) = \frac{2c_{44(2)}}{c_{44(1)} + c_{44(2)}} \cdot \frac{Q}{z - z_0} + \frac{2c_{44(2)}}{c_{44(1)} + c_{44(2)}} \cdot \Gamma \tag{42}$$

$$\Phi_2(z) = \frac{Q}{z - z_0} + \frac{(c_{44(2)} - c_{44(1)})\bar{Q}}{c_{44(1)} + c_{44(2)}} \cdot \left(\frac{1}{z - z^*} - \frac{1}{z}\right) + \Gamma - \frac{(c_{44(2)} - c_{44(1)})}{c_{44(1)} + c_{44(2)}} \cdot \frac{a^2}{z^2}\bar{\Gamma}. \tag{43}$$

When $Q = \frac{b}{2\pi i}$, Eqs. (42) and (43) are in accord with the well-known solution of Smith [26] and reduced result of Kattis and Providas [22]. And when $\Gamma = 0$ and $Q = -\frac{p}{2\pi c_{44(2)}}$, complex potential functions (42) and (43) are identical to the results of Liu [27].

It is meaningful that, by the use of Eqs. (37) and (38), one can get the solution for a planar anti-crack or rigid line in rectilinearly anisotropic materials. For the convenience of comparing with previous known solutions of a planar rigid line lies on x-axis, the tips of the circular rigid line are assumed at $c_1 = ae^{i(\pi/2-\alpha)}$ and $d_1 = ae^{i(\pi/2+\alpha)}$. Letting $a \to \infty, \alpha \to 0$ and keeping $a \sin\alpha = l$ (l denoting the half length of straight rigid line), a situation cannot exist with the shear stress at infinity [26] and the appropriate complex potentials due solely to a anti-plane singularity are

$$\Phi_1(\xi_1) = m\left[\frac{Q}{\xi_1 - \xi_0} - \frac{\bar{Q}}{\xi_1 - \bar{\xi}_0}\right] - m\left[\frac{Q\sqrt{\xi_0^2 - l^2}}{\xi_1 - \xi_0} - \frac{\bar{Q}\sqrt{\bar{\xi}_0^2 - l^2}}{\xi_1 - \bar{\xi}_0} + \bar{Q} + Q\right] \cdot \frac{1}{\sqrt{\xi^2 - l^2}} \tag{44}$$

$$\Phi_2(\xi_2) = \frac{m\beta_1}{\beta_2}\left[\frac{Q}{\xi_2 - \xi_0} - \frac{\bar{Q}}{\xi_2 - \bar{\xi}_0}\right] + m\left[\frac{Q\sqrt{\xi_0^2 - l^2}}{\xi_1 - \xi_0} - \frac{\bar{Q}\sqrt{\bar{\xi}_0^2 - l^2}}{\xi_1 - \bar{\xi}_0} + \bar{Q} + Q\right] \cdot \frac{1}{\sqrt{\xi^2 - l^2}}. \tag{45}$$

This is a new result. Assuming the materials of the upper and lower half-plane are two dissimilar isotropic media, and when $Q = -\frac{p}{2\pi c_{44(2)}}$ and $Q = \frac{b}{2\pi i}$, Eqs. (44) and (45) coincide, respectively, with the solution of Jiang and Cheung [7] and reduced result of Xiao et al. [17].

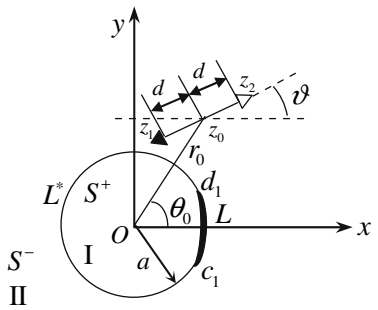

Fig. 2 A screw dislocation dipole interacting with an interfacial anti-crack model

In addition, the solution presented as Eqs. (37) and (38) is valid for either matrix is isotropic but inhomogeneity is anisotropic or matrix is anisotropic but inhomogeneity is isotropic. Moreover, when $c_{44(1)} = c_{55(1)} = c_{45(1)} = 0$ or $c_{44(1)} = c_{55(1)} = \infty, c_{45(1)} = 0$, the solutions for a anti-plane singularity interacting with a hole or a rigid inclusion in anisotropic material can be simply lead to. Here the details are omitted for saving space.

5 Screw dislocation dipole

Equations (37)–(38) are the explicit expressions of Green's functions for the current model subjected to a single anti-plane singularity located in the matrix. The solutions for two or more anti-plane singularities in the matrix can be constructed easily by the superposition of Green's functions. We consider two screw dislocations which are close to each other with Burgers vectors $b_1(= b)$ and $b_2(= -b)$ (they are also called a screw dislocation dipole), respectively, interacting with an interface anti-crack in cylindrically anisotropic solids under free loads at infinity. Referring to Fig. 2, assume that the center of the dislocation dipole with arm length $2d$ is $z_0 = r_0 e^{i\theta_0}$, then the two dislocations are located at $z_1 = z_0 - de^{i\vartheta}$ and $z_2 = z_0 + de^{i\vartheta}$, and the interfacial anti-crack symmetrically placed with respect to the x-axis and the tips of which are located at $c_1 = ae^{-i\alpha}$ and $d_1 = ae^{i\alpha}$. It indicates that $X_0(\xi)$ takes the same form as Sect. 4.

Taking Eqs. (37)–(38) into account, no matter the screw dipole emitted from the anti-crack or generated elsewhere, one can write the complex potentials in two regions as

$$\begin{aligned}\Phi_1(\xi_1) = {} & \frac{mb}{2\pi i}\left[\frac{\xi_{10}-\xi_{20}}{(\xi_1-\xi_{10})(\xi_1-\xi_{20})} + \frac{\xi_{10}^*-\xi_{20}^*}{(\xi_1-\xi_{10}^*)(\xi_1-\xi_{20}^*)}\right] \\ & -\frac{mb}{2\pi i}\left[\frac{1}{(\xi_1-\xi_{10})X_0(\xi_{10})} - \frac{1}{(\xi_1-\xi_{20})X_0(\xi_{20})}\right. \\ & \left. + \frac{1}{(\xi_1-\xi_{10}^*)X_0(\xi_{10}^*)} - \frac{1}{(\xi_1-\xi_{20}^*)X_0(\xi_{20}^*)}\right] X_0(\xi_1) \qquad (46)\end{aligned}$$

$$\begin{aligned}\Phi_2(\xi_2) = {} & \frac{m\beta_1 b}{2\pi i\beta_2}\left[\frac{\xi_{10}-\xi_{20}}{(\xi_2-\xi_{10})(\xi_2-\xi_{20})} + \frac{\xi_{10}^*-\xi_{20}^*}{(\xi_2-\xi_{10}^*)(\xi_2-\xi_{20}^*)}\right] \\ & +\frac{mb}{2\pi i}\left[\frac{1}{(\xi_2-\xi_{10})X_0(\xi_{10})} - \frac{1}{(\xi_2-\xi_{20})X_0(\xi_{20})}\right. \\ & \left. + \frac{1}{(\xi_2-\xi_{10}^*)X_0(\xi_{10}^*)} - \frac{1}{(\xi_2-\xi_{20}^*)X_0(\xi_{20}^*)}\right] X_0(\xi_2) \qquad (47)\end{aligned}$$

where $\xi_{k0} = (\frac{r_k}{a})^{-i\mu-1} r_k e^{i\theta_k}$ and $\xi_{k0}^* = a^2/\bar{\xi}_{k0} (k = 1, 2)$ with r_k and θ_k representing the polar radius and polar angle of z_k.

From Eqs. (46) and (47), one may also find some new results for the case similarly to Sect. 4. Here we omit the details for saving space.

6 Stress singularity near the anti-crack tips

For any anti-crack L_j, similarly to the stress intensity factors at crack tips [28,29], we define the stress singularity around the anti-crack tip $d_j = a\mathrm{e}^{i\theta_d}$ as

$$S_{\mathrm{III}} = \lim_{\rho\to 0}\sqrt{2\pi\rho}\sigma_{3r} \tag{48}$$

where ρ means the distance from the anti-crack tip along the interface.

Inserting Eq. (8) into Eq. (48) and noting $\rho = a\mathrm{d}\theta$ lead to

$$S_{\mathrm{III}} = \beta_1\sqrt{2\pi a}\,\mathrm{Re}\left[\lim_{\theta\to\theta_d}\sqrt{\theta-\theta_d}\mathrm{e}^{i\theta}\Phi_1(\xi_1)\right]. \tag{49}$$

In this section, we focus on the case of the interface containing a single anti-crack. Considering the anti-crack tip d_1, then substituting Eqs. (37) and (46) into Eq. (49), respectively, lead to

$$\begin{aligned} S_{\mathrm{III}} = \mathrm{Re}\Bigg\{&\beta_1 m\sqrt{\pi a\,\sin\alpha}(\Gamma\mathrm{e}^{i\alpha/2}+\bar{\Gamma}\mathrm{e}^{-i\alpha/2}) - \frac{\sqrt{\pi}\beta_1 m\mathrm{e}^{i\alpha/2}}{i\sqrt{a\,\sin\alpha}}\left[\frac{Q}{(a\mathrm{e}^{i\alpha}-\xi_0)X_0(\xi_0)}\right.\\ &\left.-\frac{\bar{Q}}{(a\mathrm{e}^{i\alpha}-\xi^*)X_0(\xi^*)}+\bar{Q}\mathrm{e}^{-i\alpha}+Q\right]\Bigg\} \end{aligned} \tag{50}$$

for anti-plane singularity and load at infinity, and

$$\begin{aligned} S_{\mathrm{III}} = \mathrm{Re}\Bigg\{&\frac{\beta_1 m\mathrm{e}^{i\alpha/2}b}{2\sqrt{\pi a\,\sin\alpha}}\left[\frac{1}{(a\mathrm{e}^{i\alpha}-\xi_{10})X_0(\xi_{10})}-\frac{1}{(a\mathrm{e}^{i\alpha}-\xi_{20})X_0(\xi_{20})}+\frac{1}{(a\mathrm{e}^{i\alpha}-\xi_{10}^*)X_0(\xi_{10}^*)}\right.\\ &\left.-\frac{1}{(a\mathrm{e}^{i\alpha}-\xi_{20}^*)X_0(\xi_{20}^*)}\right]\Bigg\} \end{aligned} \tag{51}$$

for screw dislocation dipole and absent load at infinity.

Similarly, the stress singularity near the crack tip c_1 can be obtained.

7 Image forces and image torques

When the anti-plane singularity reduces to a screw dislocation, it is necessary to investigate the image force on the dislocation due to which is a significant physical quantum for understanding interacting mechanism in studying the interaction effects of dislocation and inhomogeneity. According to Peach–Koehler formula [30] and noting the resolution of Cartesian to polar, the force exerted on a screw dislocation is given by polar form

$$F_r - iF_\theta = ib[\tilde{\sigma}_{3r}(\xi_0) - i\tilde{\sigma}_{3\theta}(\xi_0)] \tag{52}$$

where $\tilde{\sigma}_{3r}(\xi_0)$ and $\tilde{\sigma}_{3\theta}(\xi_0)$ are the perturbation stress components at the dislocation which are obtained by subtracting those attributed to the dislocation in the corresponding infinite homogeneous medium from the current stress field, then taking the limit for ξ approaching ξ_0. Considering the interface containing one

anti-crack, the components of image force are found to be

$$F_r = \frac{mb}{r_0}\,\mathrm{Re}\left\{\mu_2\xi_0\left[\frac{\beta_1 b}{2\pi i}\left(\frac{1}{\xi_0-\xi^*}-\frac{1}{\xi_0}\right)+\frac{\beta_2 b}{2\pi i}\left[\frac{1}{(\xi_0-\xi^*)X_0(\xi^*)}-\frac{a}{\xi_0}+1\right]X_0(\xi_0)\right.\right.$$
$$\left.\left.-\frac{\beta_2 b}{2\pi i}(\xi_0-a\,\cos\alpha)X_0^2(\xi_0)+\beta_2\left(\frac{a^3}{\xi_0^2}\bar{\Gamma}-\frac{a^2}{\xi_0}\bar{\Gamma}\,\cos\alpha+\Gamma\xi_0-\Gamma a\,\cos\alpha\right)X_0(\xi_0)+\beta_1\left(\Gamma+\frac{a^2}{\xi_0^2}\bar{\Gamma}\right)\right]\right\} \tag{53}$$

$$F_\theta = -\frac{mb}{r_0}\,\mathrm{Re}\left\{\xi_0\left[\frac{\beta_1 b}{2\pi i}\left(\frac{1}{\xi_0-\xi^*}-\frac{1}{\xi_0}\right)+\frac{\beta_2 b}{2\pi i}\left[\frac{1}{(\xi_0-\xi^*)X_0(\xi^*)}-\frac{a}{\xi_0}+1\right]X_0(\xi_0)\right.\right.$$
$$\left.\left.-\frac{\beta_2 b}{2\pi i}\frac{\xi_0-a\,\cos\alpha}{X_0^2(\xi_0)}+\beta_2\left(\frac{a^3}{\xi_0^2}\bar{\Gamma}-\frac{a^2}{\xi_0}\bar{\Gamma}\,\cos\alpha+\Gamma\xi_0-\Gamma a\,\cos\alpha\right)X_0(\xi_0)+\beta_1\left(\Gamma+\frac{a^2}{\xi_0^2}\bar{\Gamma}\right)\right]\right\}. \tag{54}$$

Referring to the work of Juang and Lee [31], the image force components F_{0r} and $F_{0\theta}$ and image torque T acting on the center of screw dislocation under consideration are possible to be arrived at

$$F_{0r} = F_{1r}\,\cos(\theta_1-\theta_0)+F_{2r}\,\cos(\theta_0-\theta_2)-F_{1\theta}\,\sin(\theta_1-\theta_0)+F_{2\theta}\,\sin(\theta_0-\theta_2) \tag{55}$$
$$F_{0\theta} = F_{1r}\,\sin(\theta_1-\theta_0)-F_{2r}\,\sin(\theta_0-\theta_2)+F_{1\theta}\,\cos(\theta_1-\theta_0)+F_{2\theta}\,\cos(\theta_0-\theta_2) \tag{56}$$
$$T = [F_{1r}\,\sin(\theta_1-\vartheta)-F_{2r}\,\sin(\theta_2-\vartheta)+F_{1\theta}\,\cos(\theta_1-\vartheta)-F_{2\theta}\,\cos(\theta_2-\vartheta)]d \tag{57}$$

where F_{kr} and $F_{k\theta}(k=1,2)$ are image force components exerted on dislocation at z_k, respectively; and they can be derived from Eq. (52) as

$$F_{1r} = \frac{mb^2}{2\pi r_1}\,\mathrm{Re}\left\{-i\mu_2\xi_{10}\left[\beta_1\left(-\frac{1}{\xi_{10}-\xi_{20}}+\frac{1}{\xi_{10}-\xi_{10}^*}-\frac{1}{\xi_{10}-\xi_{20}^*}\right)+\beta_2\left[-\frac{1}{(\xi_{10}-\xi_{20})X_0(\xi_{20})}\right.\right.\right.$$
$$\left.\left.\left.+\frac{1}{(\xi_{10}-\xi_{10}^*)X_0(\xi_{10}^*)}-\frac{1}{(\xi_{10}-\xi_{20}^*)X_0(\xi_{20}^*)}\right]\cdot X_0(\xi_{10})-\beta_2(\xi_{10}-a\,\cos\alpha)X_0^2(\xi_{10})\right]\right\} \tag{58}$$
$$F_{1\theta} = \frac{mb^2}{2\pi r_1}\,\mathrm{Re}\left\{i\xi_{10}\left[\beta_1\left(-\frac{1}{\xi_{10}-\xi_{20}}+\frac{1}{\xi_{10}-\xi_{10}^*}-\frac{1}{\xi_{10}-\xi_{20}^*}\right)+\beta_2\left[-\frac{1}{(\xi_{10}-\xi_{20})X_0(\xi_{20})}\right.\right.\right.$$
$$\left.\left.\left.+\frac{1}{(\xi_{10}-\xi_{10}^*)X_0(\xi_{10}^*)}-\frac{1}{(\xi_{10}-\xi_{20}^*)X_0(\xi_{20}^*)}\right]\cdot X_0(\xi_{10})-\beta_2(\xi_{10}-a\,\cos\alpha)X_0^2(\xi_{10})\right]\right\} \tag{59}$$
$$F_{2r} = \frac{mb^2}{2\pi r_2}\,\mathrm{Re}\left\{i\mu_2\xi_{20}\left[\beta_1\left(\frac{1}{\xi_{20}-\xi_{10}}+\frac{1}{\xi_{20}-\xi_{10}^*}-\frac{1}{\xi_{20}-\xi_{20}^*}\right)+\beta_2\left[\frac{1}{(\xi_{20}-\xi_{10})X_0(\xi_{10})}\right.\right.\right.$$
$$\left.\left.\left.+\frac{1}{(\xi_{20}-\xi_{10}^*)X_0(\xi_{10}^*)}-\frac{1}{(\xi_{20}-\xi_{20}^*)X_0(\xi_{20}^*)}\right]\cdot X_0(\xi_{20})+\beta_2(\xi_{20}-a\,\cos\alpha)X_0^2(\xi_{20})\right]\right\} \tag{60}$$
$$F_{2\theta} = -\frac{mb^2}{2\pi r_2}\,\mathrm{Re}\left\{i\xi_{20}\left[\beta_1\left(\frac{1}{\xi_{20}-\xi_{10}}+\frac{1}{\xi_{20}-\xi_{10}^*}-\frac{1}{\xi_{20}-\xi_{20}^*}\right)+\beta_2\left[\frac{1}{(\xi_{20}-\xi_{10})X_0(\xi_{10})}\right.\right.\right.$$
$$\left.\left.\left.+\frac{1}{(\xi_{20}-\xi_{10}^*)X_0(\xi_{10}^*)}-\frac{1}{(\xi_{20}-\xi_{20}^*)X_0(\xi_{20}^*)}\right]\cdot X_0(\xi_{20})+\beta_2(\xi_{20}-a\,\cos\alpha)X_0^2(\xi_{20})\right]\right\}. \tag{61}$$

8 Numerical analysis and discussion

Taking the case of one interfacial anti-crack and free load at infinity for example, we focus on the stress singularities at the anti-crack tips and image forces exerted on the screw dislocation in the following. It is assumed that the anti-plane singularity or the center of screw dislocation dipole locate on x-axis and materials are orthotropic, the latter means $\mu = i\sqrt{c_{44}/c_{55}}$. Denote $\eta = \sqrt{c_{44}/c_{55}}$, which represents the extent of

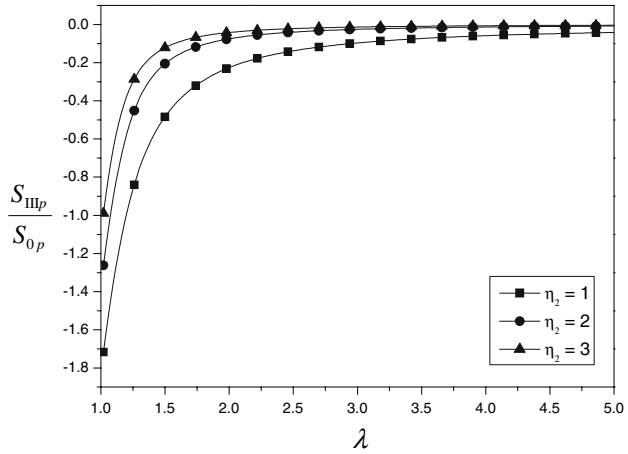

Fig. 3 Normalized stress singularities $S_{\mathrm{III}p}$ versus λ with different η_2 for $\eta_1 = 2$ and $\alpha = 30°$

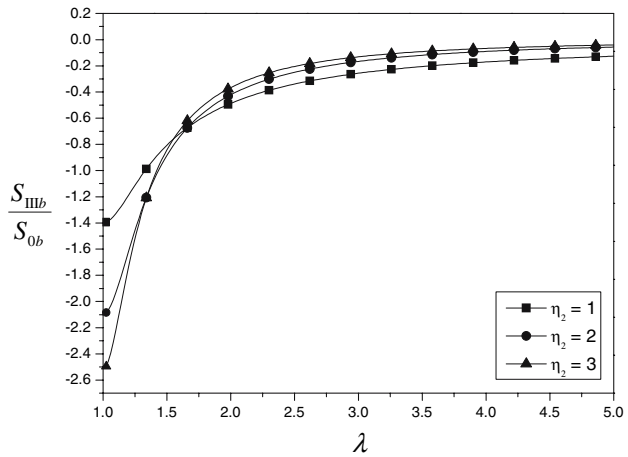

Fig. 4 Normalized stress singularities $S_{\mathrm{III}b}$ versus λ with different η_2 for $\eta_1 = 2$ and $\alpha = 30°$

anisotropy of material and dimensionless distance $\lambda = r_0/a$. In addition, $c_{55(2)}/c_{55(1)}$ is restricted to constant one for giving prominence to the influence of anisotropy upon stress singularities and image forces. Introduce the following parameters to scale the stress singularities and image forces:

$$S_{0p} = \frac{p}{2\sqrt{\pi a}}, \quad S_{0b} = \frac{c_{55}b}{2\sqrt{\pi a}}, \quad F_0 = \frac{c_{55}b^2}{2\pi a}.$$

Figures 3, 4, 5 and 6 illustrate the influence of anisotropies of materials upon stress singularities near the anti-crack tip. Normalized stress singularities $S_{\mathrm{III}p}$ and $S_{\mathrm{III}b}$ versus λ with different η_2 for $\eta_1 = 2$ and $\alpha = 30°$ are depicted in Figs. 3 and 4, respectively. It can be observed that, with the increment of distance between the singularity and interface anti-crack, the stress singularities around the anti-crack decrease monotonically, and the singularity shields the anti-crack regardless of the anisotropies of materials. When the screw dislocation is close to the anti-crack, the anisotropy ratio of matrix material may enhance the shielding effect, but when the screw dislocation is far from the anti-crack in some sort, this trend is reversed. However, in the process of the anti-plane concentrated force approaching the interfacial anti-crack from infinity, the anisotropy ratio of material may weaken the stress singularities. Figures 5 and 6 show the variations of normalized stress singularities $S_{\mathrm{III}p}$ and $S_{\mathrm{III}b}$ versus α with different η_2 for $\eta_1 = 2$ and $\lambda = 1.2$. The magnitude of normalized stress singularities decrease firstly and then augment with the increase of anti-crack angle. There are different minimal values in the turning points and for which the shielding effects is strongest. Noticeably, the anisotropy properties of materials may weaken the stress singularity near the anti-crack tip for the singularity being a concentrated force but enhance the one for the singularity being a screw dislocation.

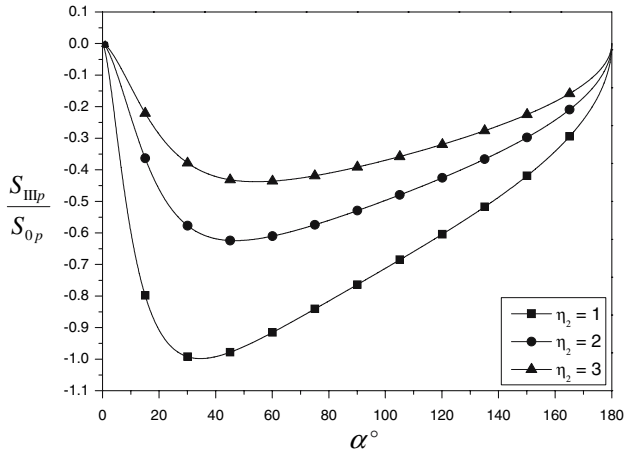

Fig. 5 Normalized stress singularities $S_{\mathrm{III}p}$ versus α with different η_2 for $\eta_1 = 2$ and $\lambda = 1.2$

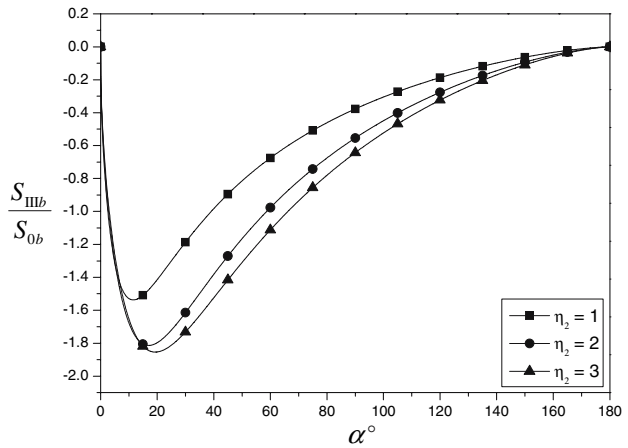

Fig. 6 Normalized stress singularities $S_{\mathrm{III}b}$ versus α with different η_2 for $\eta_1 = 2$ and $\lambda = 1.2$

For the case of a screw dislocation dipole near the interfacial anti-crack, Fig. 7 describes the variations of normalized stress singularities $S_{\mathrm{III}d}$ versus dipole orientation ϑ with different η_2 for $\eta_1 = 2$, $\alpha = 30^\circ$ and $\lambda = 1.2$. As can be seen, when the two components of screw dislocation dipole are symmetrically located with respect to x-axis ($\vartheta = 90^\circ$ or 270°), the magnitude of the stress singularities are equal to zero, and the stress singularities possess the biggest negative values when $\vartheta = 0^\circ(360^\circ)$ and the ultimate positive values when $\vartheta = 180^\circ$. In addition, the anisotropy ratios may enhance the singular effect of dislocation dipole acting on the anti-crack tip.

Due to the screw dislocation locates on x-axis, the tangential component of image force reduce to zero. We focus on the remaining radial component of image force. Normalized radial image forces F_r versus λ with different η_2 for $\eta_1 = 2$ and $\alpha = 10^\circ$ are plotted in Fig. 8. It can be seen that when the screw dislocation approaches the interface along x-axis from infinity, the inhomogeneity and interface anti-crack always repel the screw dislocation if the anisotropy ratios of matrix are less or equal to the inhomogeneity's; however, if the matrix's anisotropy ratios larger than inhomogeneity's, the inhomogeneity and interfacial anti-crack attract the screw dislocation firstly and then repel it. There is a stable equilibrium position at which the image force equals to zero. Figure 9 shows the variations of normalized radial image forces F_r versus α with different η_2 for $\eta_1 = 2$ and $\lambda = 1.2$. It is found that the radial image forces increase with the increment of the anti-crack angle and become constant values after the anti-crack reaches certain length. When $\alpha = 0^\circ$, namely, the anti-crack vanishes, the inhomogeneity attracts the screw dislocation inside the matrix with larger anisotropy than inhomogeneity's when it repels the dislocation in the matrix with smaller anisotropy.

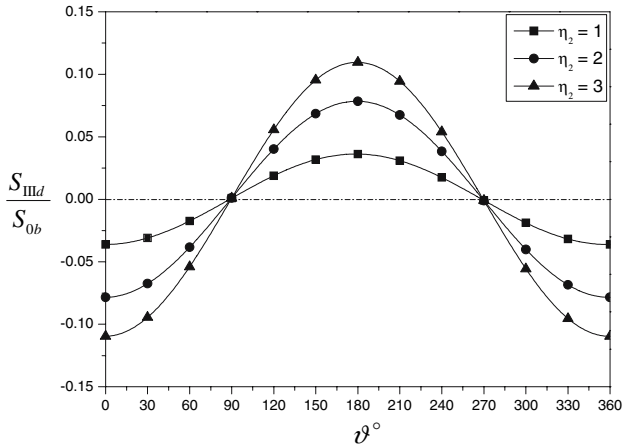

Fig. 7 Normalized stress singularities $S_{\mathrm{III}d}$ versus ϑ with different η_2 for $\eta_1 = 2$, $\alpha = 30^\circ$ and $\lambda = 1.2$

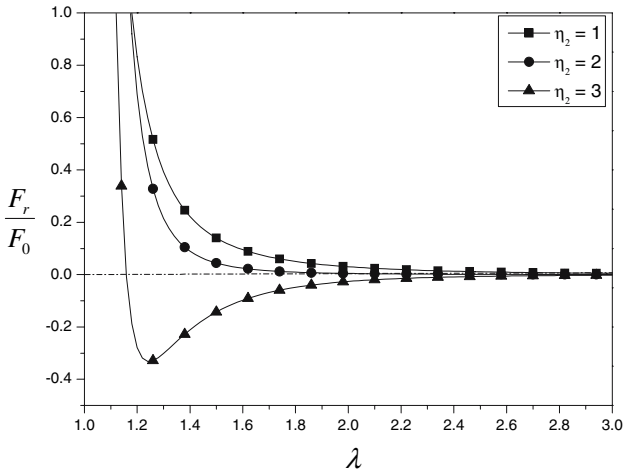

Fig. 8 Normalized radial image forces F_r versus λ with different η_2 for $\eta_1 = 2$ and $\alpha = 10^\circ$

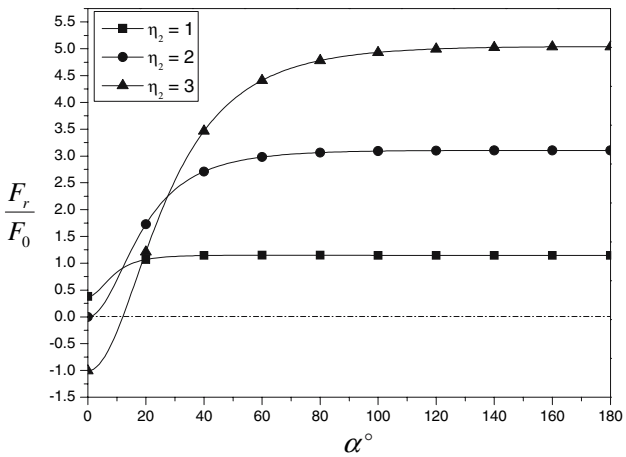

Fig. 9 Normalized radial image forces F_r versus α with different η_2 for $\eta_1 = 2$ and $\lambda = 1.2$

9 Conclusions

The interaction between an anti-plane singularity and interfacial anti-cracks in cylindrically anisotropic composites is studied in this paper. By employing a complex potential technique, we obtain the general solution of this problem. Particularly, the closed solution for interface containing one anti-crack is presented analytically. In addition, the complex potentials for a screw dislocation dipole inside a matrix are obtained by superimposing method. Expressions of stress singularities around the anti-crack tips, image forces and torques acting on dislocation or the center of dipole are given explicitly. The results show that the anisotropies of materials have significant influence on the stress singularities and image forces. The presented solutions are valid for anisotropic, orthotropic or isotropic composites and can be reduced to some novel or previously known results.

Acknowledgments The authors appreciate the support by the National Natural Science Foundation of China (10472030).

References

1. Wang, Z.Y., Zhang, H.T., Chou, Y.T.: Stress singularity at the tip of a rigid line inhomogeneity under antiplane shear loading. ASME J. Appl. Mech. **53**, 459–461 (1986)
2. Chen, Y.Z., Cheung, Y.K: Stress singularity coefficients in an infinite plate containing rigid line and applied by concentrated forces. Eng. Fract. Mech. **26**, 729–739 (1987)
3. Cheung, Y.K., Chen, Y.Z.: Multiple rigid line problems in an infinite plate. Eng. Fract. Mech. **34**, 379–391 (1989)
4. Li, Q.Q., Ting, T.C.T.: Line inclusions in anisotropic elastic solids. ASME J. Appl. Mech. **56**, 556–563 (1989)
5. Ballarini, R.: A rigid line inclusion at a bimaterial interface. Eng. Fract. Mech. **37**, 1–5 (1990)
6. Fan, H., Keer, L.M.: Two-dimensional line defects in anisotropic elastic solids. Int. J. Fract. **62**, 25–42 (1993)
7. Jiang, C.P., Cheung, Y.K.: Antiplane problems of collinear rigid line inclusions in dissimilar media. Eng. Fract. Mech. **52**, 907–915 (1995)
8. Asundi, A., Deng, W.: Rigid inclusions on the interface between dissimilar anisotropic media. J. Mech. Phys. Solids **43**, 1045–1058 (1995)
9. Chen, Y.Z., Hasebe, N.: Properties of eigenfunction expansion form for the rigid line problem in dissimilar media. Int. J. Solids Struct. **33**, 611–628 (1996)
10. Wu, L.Z., Du, S.Y.: A rigid line in a confocal elliptic piezoelectric inhomogeneity embedded in an infinite piezoelectric medium. Int. J. Solids Struct. **37**, 1453–1469 (2000)
11. Chen, B.J., Xiao, Z.M., Liew, K.M.: On the interaction between a semi-infinite anti-crack and a screw dislocation in piezoelectric solid. Int. J. Solids Struct. **39**, 1505–1513 (2002)
12. Xiao, Z.M., Dai, Y., Chen, B.J.: Micro-crack initiation at tip of a rigid line inhomogeneity in piezoelectric materials. Int. J. Eng. Sci. **41**, 137–147 (2003)
13. Liu, Y.W., Fang, Q.H.: Electro-elastic interaction between a piezoelectric screw dislocation and circular interfacial rigid lines. Int. J. Solids Struct. **40**, 5353–5370 (2003)
14. Fang, Q.H., Liu, Y.W., Jiang, C.P.: On the interaction between a generalized screw dislocation and circular-arc interfacial rigid lines in magnetoelectroelastic solids. Int. J. Eng. Sci. **43**, 1011–1031 (2005)
15. Xiao, Z.M., Zhang, H.X., Chen, B.J.: Micro-crack initiation at the tip of a semi-infinite rigid line inhomogeneity in piezoelectric solids. Int. J. Eng. Sci. **43**, 1223–1233 (2005)
16. Prasad, P.B.N., Hasebe, N., Wang, X.F., Shirai, Y.: Green's functions for a bi-material problem with interfacial elliptical rigid inclusion and applications to crack and thin rigid line problems. In. J. Solids Struct. **42**, 1513–1535 (2005)
17. Xiao, Z.M., Zhang, H.X., Chen, B.J.: A piezoelectric screw dislocation interacts with interfacial collinear rigid lines in piezoelectric bimaterials. Int. J. Solids Struct. **44**, 255–271 (2007)
18. Yang, S., Yuan, F.G.: Interfacial circular crack in cylindrically anisotropic composites under antiplane shear. Int. J. Solids Struct. **32**, 3603–3628 (1995)
19. Ting, T.C.T.: Pressuring, shearing, torsion and extension of a circular tube or bar of cylindrically anisotropic material. Proc. R. Soc. Lond. A **452**, 2397–2421 (1996)
20. Ting, T.C.T.: The remarkable nature of cylindrically anisotropic elastic materials exemplified by an anti-plane deformation. J. Elast. **49**, 269–284 (1998)
21. Suo, Z.: Singularities, interfaces and cracks in dissimilar anisotropic media. Proc. R. Soc. Lond. A **427**, 331–358 (1990)
22. Kattis, M.A., Providas, E.: Two-phase potentials in anisotropic elasticity: antiplane deformation. Int. J. Eng. Sci. **36**, 801–811 (1998)
23. Lee, K.W., Lim, J.H., Earmme, Y.: A screw dislocation interacting with an interfacial crack in two anisotropic thin films with finite thickness. Mech. Mater. **33**, 97–103 (2001)
24. Muskhelishvili, N.L.: Some Basic Problems of Mathematical Theory of Elasticity. Noordhoff, Leyden (1975)
25. Shin, H., Earmme, Y.Y.: Interaction of screw dislocation and anisotropic (or isotropic) circular inclusion in isotropic (or anisotropic) matrix. Int. J. Fract. **126**, L35–L40 (2004)
26. Smith, E.: The interaction between dislocations and inhomogeneities—I. Int. J. Eng. Sci. **6**, 129–143 (1968)
27. Liu, Y.W.: Basis singular solutions of anti-plane problem on circular-arc cracks between bonded dissimilar materials. Acta Mech. Solid. Sin. **12**, 244–254 (1991)

28. Gao, C.F., Balke, H.: Fracture analysis of circular-arc interface cracks in piezoelectric materials. Int. J. Solids Struct. **40**, 3507–3522 (2003)
29. Gao, C.F., Kessler, H., Balke, H.: Green's functions for anti-plane deformations of a circular arc-crack at the interface of piezoelectric materials. Arch. Appl. Mech. **73**, 467–480 (2003)
30. Hirth, J.P., Lothe, J.: Theory of Dislocations. Wiley, New York (1982)
31. Juang, R.R., Lee, S.: Elastic interaction between general parallel screw dislocations and a surface crack. J. Appl. Phys. **59**, 3421–3429 (1986)